Article:

Malavelle, FF, Haywood, JM, Jones, A et al. (31 more authors) (2017) Strong constraints on aerosol–cloud interactions from volcanic eruptions. Nature, 546 (7659). pp. 485-491. ISSN 0028-0836

https://doi.org/10.1038/nature22974

Strong constraints on aerosol-cloud interactions from volcanic eruptions

Authors: Florent F. Malavelle[1*], Jim M. Haywood[1,2], Andy Jones[2], Andrew Gettelman[3], Lieven Clarisse[4], Sophie Bauduin[4], Richard P. Allan[5,6], Inger Helene H. Karset[7], Jón Egill Kristjánsson[7,$], Lazaros Oreopoulos[8], Nayeong Cho[8,9], Dongmin Lee[8,10], Nicolas Bellouin[5], Olivier Boucher[11], Daniel P. Grosvenor[12], Ken S. Carslaw[12], Sandip Dhomse[12], Graham W. Mann[12,13], Anja Schmidt[12], Hugh Coe[14], Margaret E. Hartley[14], Mohit Dalvi[2], Adrian A. Hill[2], Ben T. Johnson[2], Colin E. Johnson[2], Jeff R. Knight[2], Fiona M. O'Connor[2], Daniel G. Partridge[15,16,17,#], Philip Stier[17], Gunnar Myhre[18], Steven Platnick[8], Graeme L. Stephens[19], Hanii Takahashi[20,19], Thorvaldur Thordarson[21].

Affiliations:

[1]College of Engineering, Mathematics, and Physical Sciences, University of Exeter, Exeter, UK.

[2]Met Office Hadley Centre, Exeter, UK.

[3]National Center for Atmospheric Research, Boulder, Colorado, USA.

[4]Chimie Quantique et Photophysique CP160/09, Université Libre de Bruxelles (ULB), Bruxelles, Belgium.

[5]Department of Meteorology, University of Reading, Reading, UK.

[6]National Centre for Earth Observation, University of Reading, UK.

[7]Department of Geosciences, University of Oslo, Oslo, Norway.

[8]Earth Sciences Division, NASA GSFC, Greenbelt, Maryland, USA.

[9]USRA, Columbia, Maryland, USA.

[10]Morgan State University, Baltimore, Maryland, USA.

[11]Laboratoire de Météorologie Dynamique, IPSL, UPMC/CNRS, Jussieu, France.

[12]School of Earth and Environment, University of Leeds, Leeds, UK.
[13]National Centre for Atmospheric Science, University of Leeds, Leeds, UK.
[14]School of Earth and Environmental Sciences, University of Manchester, Manchester, UK.
[15]Department of Environmental Science and Analytical Chemistry, University of Stockholm, Stockholm, Sweden
[16]Bert Bolin Centre for Climate Research, University of Stockholm, Stockholm, Sweden
[17]Atmospheric, Oceanic and Planetary Physics, Department of Physics, University of Oxford, Oxford, UK.
[18]Center for International Climate and Environmental Research, Oslo, Norway.
[19]Jet Propulsion Laboratory, California Institute of Technology, Pasadena, California, USA.
[20]Joint Institute for Regional Earth System Science and Engineering, University of California, Los Angeles, California, USA
[21]Faculty of Earth Sciences, University of Iceland, Reykjavik, Iceland.

[*]Corresponding author: f.malavelle@exeter.ac.uk
[$]Deceased 14th August 2016.
[#]Now at College of Engineering, Mathematics, and Physical Sciences, University of Exeter, Exeter, UK.

Summary (149 words of referenced text):

The climate impact of aerosols is highly uncertain owing primarily to their poorly quantified influence on cloud properties. During 2014-15, a fissure eruption in Holuhraun (Iceland) emitted huge quantities of sulphur dioxide, resulting in significant reductions in liquid cloud droplet size. Using satellite observations and detailed modelling, we estimate a global mean radiative forcing from the resulting aerosol-induced cloud brightening for the time of the eruption of around -0.2 $W.m^{-2}$. Changes in cloud amount or liquid water path are undetectable, indicating that these aerosol-cloud indirect effects are modest. It supports the

idea that cloud systems are well buffered against aerosol changes as only impacts on cloud effective radius appear relevant from a climate perspective, thus providing a strong constraint on aerosol-cloud interactions. This result will reduce uncertainties in future climate projections as we are able to reject the results from climate models with an excessive liquid water path response.

Main Text: (3103 words of referenced text, including concluding paragraph)

1. The 2014-15 eruption at Holuhraun (486 words of referenced text):

Anthropogenic emissions that affect climate are not just confined to greenhouse gases. Sulphur dioxide and other pollutants form atmospheric aerosols that can scatter and absorb sunlight and can influence the properties of clouds, modulating the Earth-atmosphere energy balance. Aerosols act as cloud condensation nuclei (CCN); an increase in CCN translates into a higher number of smaller, more reflective cloud droplets that scatter more sunlight back to space[1] (the 'first' indirect effect of aerosols). Smaller cloud droplets decrease the efficiency of collision-coalescence processes that are pivotal in rain initiation, thus aerosol-influenced clouds may retain more liquid water and extend coverage/lifetime[2,3] (the 'second' or 'cloud lifetime' indirect effect). Aerosols usually co-vary with key environmental variables making it difficult to disentangle aerosol-cloud impacts from meteorological variability[4-6]. Additionally, clouds themselves are complex transient systems subject to dynamical feedbacks (e.g. cloud top entrainment/evaporation, invigoration of convection) which influence cloud response[7-12]. These aspects present great challenges in evaluating and constraining aerosol-cloud interactions (ACI) in General Circulation Models (GCM)[13-17], with particular contentious debate surrounding the relative importance of these feedback mechanisms.

Nonetheless, anthropogenic aerosol emissions are thought to cool the Earth via indirect effects[17], but the uncertainty ranges from -1.2 to -0.0 $W.m^{-2}$ (90% confidence interval) due to *i)* a lack of characterization of the pre-industrial aerosol state[15,18,19], and *ii)* model parametric and structural errors in representing cloud responses to aerosol changes[16,18,20,21]. It is estimated that uncertainty in the pre-industrial state can account for approximately 30% of total ACI uncertainty[18,21] while representation of chemistry-aerosol-cloud processes in models is responsible for the remaining 70% uncertainty[16,21]. Recently, a framework to break down uncertainties in the causal chain from emission to radiative forcing showed that the sources of uncertainty within different GCMs differ greatly[16].

Volcanic eruptions provide invaluable natural experiments to investigate the role of large-scale aerosol injection in the Earth system[22-26]. There have been several Icelandic volcanic eruptions over recent years; Eyjafjallajökull erupted in 2010, Grímsvötn in 2011 and Holuhraun in 2014-15. At its peak, the 2014-15 eruption at Holuhraun emitted ~120 kt of sulphur dioxide (SO_2) per day into the atmosphere, a rate some four times higher than all 28 European Union member states or over a third of global emission rates. Iceland became in effect a continental-scale pollution source of SO_2; SO_2 is readily oxidised via gas- and aqueous-phase reactions, producing a massive aerosol plume in a near-pristine environment where clouds should be most susceptible to aerosol concentrations[16,18,27].

We advance upon preliminary observational assessments of the impact of the 2014-15 eruption at Holuhraun[28,29] through an extensive observational analysis that includes a statistical evaluation of the significance of the observed spatial distribution of the cloud perturbations to untangle the impacts of aerosol/meteorological impacts. We then assess the simulation from a range of different climate models and assess the performance against available observations. Finally, we show that observations of a volcanic plume (Mt. Kilauea, Hawaii) in an entirely different meteorological regime exhibit similar overall impacts.

2. Impact of the eruption on clouds (2140 - 20 = 2120 words of referenced text):

Following the lifecycle of sulphur from emission, our initial analysis concentrates on the coherence of SO_2 detected by the Infrared Atmospheric Sounding Interferometer (IASI) sensor (Supplementary M1) and the HadGEM3 GCM that is constrained by observed temperatures and winds (i.e. nudged, Supplementary M2). IASI retrievals use the discrete spectral absorption structure of SO_2 to determine concentrations[30]. Comparisons of IASI SO_2 observations from explosive volcanic eruptions against model simulations have proven valuable in the past[31,32]. The processing procedure for quantitative comparison between IASI and HadGEM3 data uses only data that are spatially and temporally coherent (Supplementary M3).

There is considerable uncertainty in the quantitative emission of SO_2 from the 2014-15 eruption at Holuhraun. A previous study[28] assumed a constant emission rate of 40 kt[SO_2]/day based on initial estimates of degassing. As our standard scenario (STAN) we use an empirical relationship between degassed sulphur and TiO_2/FeO ratios and lava production derived from Icelandic basaltic flood lava eruptions[33] which suggests significantly higher emissions during the early phase of the eruption in September, but we also investigate a simulation where a constant 40 ktSO_2/day is released (40KT scenario). The model simulations and IASI retrievals of column SO_2 are shown in Figure 1 (40KT emission scenario shown in Supplementary S1).

Insert Figure 1 here

The distribution and the magnitude of the column loading of SO_2 detected by IASI are similar to those derived from HadGEM3, showing that the GCM nudging scheme and the assumed altitude of the emissions in the STAN scenario (surface to 3 km) reproduces the week to week spatial variability and magnitude of observed column SO_2 (SI-SO2_animation.mp4). While the spatial distribution of sulphate aerosol optical depth (*AOD*) caused by the eruption can be determined easily in the model (Supplementary Fig. S2.1), detection of the aerosol plume over the north Atlantic in the MODIS data is hampered by the mutual exclusivity of aerosol and cloud retrievals. The predominance of cloudy scenes makes accurate detection of the aerosol plume in monthly-mean MODIS data extremely challenging (Supplementary S2).

Nonetheless, despite lacking observations of *AOD*, we can look for evidence of perturbations caused by aerosols on cloud properties. We examine the perturbation to retrieved cloud top droplet effective radius (r_{eff}) in September and October 2014 using collection 051 monthly mean data from MODIS AQUA (MYD08, Supplementary M4) over the period 2002-2014. MODIS AQUA data are not subject to the degradation in performance of the sensors at visible wavelengths that has recently been documented for the MODIS TERRA[34] sensor (Supplementary S3). We present a summary of the change in r_{eff}, Δr_{eff}, for October 2014 compared to the long term 2002-2013 mean in Figure 2a. A full analysis of the year-to-year variability in Δr_{eff} is presented in Supplementary S4.

******Insert Figure 2 here******

There is clear evidence of a signal in Δr_{eff} in October (Figures 2a) and September (Supplementary Fig. S5.1a). Pixels that are statistically significantly different from the 2002-2013 climatological mean at 95% confidence occur over the entire breadth of the north Atlantic. The spatial distribution of Δr_{eff} is governed by the prevailing wind conditions that advect the volcanic plume and are quantitatively similar to those noted in Collection 006 MODIS data[29].

Figures 3a show the corresponding Δr_{eff} derived from the model in October (for September, Supplementary Fig. S5.2a). The observations and modelling show obvious similarities in spatial distribution. In addition to the spatial coherence in Δr_{eff}, the changes in the model of -1.21 μm (September) and -0.68 μm (October) are within 30% of MODIS Δr_{eff} of -0.98 μm (September) and -0.97 μm (October) for the domain shown in Figure 2.

******Insert Fig 3 here******

There are similarities between the MODIS and HadGEM3 probability distribution functions (Figures 2b and 3b) with a shift to smaller r_{eff} for the year of the eruption. Almost all high values of r_{eff} (i.e. $r_{eff} > \sim 16$ μm for MODIS and $r_{eff} > \sim 11$ μm for HadGEM3) are absent in 2014 suggesting that clouds with high r_{eff} are entirely absent from the domain in both the observations and the model. There are obvious discrepancies in the absolute magnitude of r_{eff} between MODIS and HadGEM3. MODIS retrievals of r_{eff} from the MYD06 product in liquid water cloud regimes have been shown to be significantly larger than those derived from other satellite sensor products, mainly due to the algorithm's use of a different primary spectral channel relative to other products[35,36]. Nevertheless, Δr_{eff} is in encouraging agreement as this quantity, along with changes in cloud liquid water path (*LWP*), needs to be accurately represented if aerosol-cloud interactions are to be better quantified. As with r_{eff}, there are similarities between the MODIS and HadGEM3 for ΔLWP (Figure 2c-d and Figure 3c-d), however, evidence of a clear signal due to the volcano is neither observed or modelled. Additionally, we also found that perturbations in the monthly mean cloud fraction from MODIS are negligible, both in September and October as previously reported[29].

It is incumbent on any study attributing Δr_{eff} to volcanic emissions to prove the causality beyond reasonable doubt, i.e. that the changes are not due to natural meteorological variability. The meteorological analyses in Supplementary S6 suggest that, while in September 2014 the southern part of the spatial domain shown in Figure 2 is somewhat influenced by anomalous easterlies bringing pollution from the European continent over the easternmost Atlantic Ocean and hence influencing r_{eff}, the perturbations to r_{eff} during October 2014 are entirely of volcanic origin.

MODIS and HadGEM3 show a similar spatial distribution and magnitude for October for the perturbation in cloud droplet number concentration (ΔN_d), but a smaller ΔN_d in MODIS than in HadGEM3 for September 2014 (Supplementary S7.2). Once r_{eff} is reduced, the autoconversion process whereby cloud droplets grow to sufficient size to form precipitation may be inhibited, leading to clouds with increased liquid water path[3]. The cloud optical depth, τ_{cloud}, is related to r_{eff} and LWP and the density of water (ρ) by the approximation:

$$\tau_{\mathrm{cloud}} \cong \frac{3\mathrm{LWP}}{2\rho \mathrm{r}_{\mathrm{eff}}} \quad (1)$$

We use HadGEM3 to assess the detectability of perturbations against natural variability. Two different methods are pursued using the nudged model; firstly, assessing model simulations with and without the emissions from the eruption for the year 2014 (HOL_{2014}-NO_HOL_{2014}), and secondly assessing model simulations including emissions from Holuhraun for 2014 against simulations for 2002-2013 (HOL_{2014}-$NO\_HOL_{2002\text{-}2013}$). While the former method allows the 'cleanest' assessment of the impacts of the eruption (as the meteorology is effectively identical and meteorological variability is removed), the second method allows assessment of the statistical significance against the natural meteorological variability. This provides an assessment that is directly comparable to observations and can be used to effectively isolate signal from noise[37] (Supplementary S7).

Insert Figure 4 here

Figure 4 shows that ΔAOD, ΔN_d, and Δr_{eff} are statistically significant at 95% confidence across the majority of latitudes. The fact that the simulations from [HOL_{2014}-NO_HOL_{2014}] and [HOL_{2014}-$NO\_HOL_{2002\text{-}2013}$] are similar for these variables again indicates that the impacts of natural meteorological variability on these variables is small (i.e. $NO\_HOL_{2014} \approx NO\_HOL_{2002\text{-}2013}$). For ΔLWP, no statistically significant changes are evident at either 95% or 67% confidence, suggesting that meteorological variability provides a far stronger control on cloud LWP than aerosol (Supplementary S7.3). With ΔLWP being due to meteorological noise, $\Delta\tau_{cloud}$ is driven by Δr_{eff} and Figure 4e suggests that the perturbations to τ_{cloud} north of around 67°N/57°N, which are significant at the 95%/67% confidence level, are due to the 2014-15 Holuhraun eruption. Our simulations suggest that Top of Atmosphere changes in short wave radiation (ΔToA_{SW}) are unlikely to be detectable at 95% or even 67% confidence when compared to natural variability. More details supporting this assertion are given in Supplementary S7.5 which uses satellite observations of the Earth's radiation budget.

We have shown that HadGEM3 is capable of representing observations of aerosol-cloud interactions with a reasonable representation of the perturbation to r_{eff} but minimal perturbation to *LWP*. To demonstrate the practical value of the study, we repeat the simulations with other models. First, we use HadGEM3 but using the older single moment CLASSIC[38] aerosol scheme instead of the new two-moment UKCA/GLOMAP-mode scheme[39]. We also perform calculations with the NCAR Community Atmosphere Model[28] (CAM5-NCAR) and the atmospheric component of an intermediate version of the Norwegian Earth System Model[40] (CAM5-Oslo), driven using nominally the same emissions and plume top height. CAM5-NCAR has been used previously in free-running mode to provide an initial estimate of the radiative forcing of the 2014-15 Holuhraun eruption[28], but as in the HadGEM3 simulations we run CAM5-NCAR and CAM5-Oslo in nudged mode to simulate the meteorology during the eruption as closely as possible. Figure 5 shows a comparison of Δr_{eff} and ΔLWP derived from HOL_{2014}-NO_HOL_{2014} simulations from HadGEM3, HadGEM3-CLASSIC, CAM5-NCAR, CAM5-Oslo and MODIS for October. We chose October as the contribution from continental Europe pollution to cloud property anomalies has been shown to be small (Supplementary S4-6-7; Supplementary S8 shows the impacts on cloud properties in September).

******Insert Figure 5 here******

It is immediately apparent from the first column of Figure 5 that HadGEM3 using UKCA, CAM5-NCAR, and CAM5-Oslo are able to accurately model the impact on Δr_{eff}, while HadGEM3-CLASSIC produces an impact that is too strong when compared to the MODIS observations owing to the single moment nature of the aerosol scheme (Supplementary S9).

For ΔLWP, as we have seen from the multi-year analysis of MODIS (Supplementary Fig. S7.3), the meteorological variability is the controlling factor. Even with meteorological variability suppressed in these [HOL_{2014}-NO_HOL_{2014}] results, HadGEM3 using UKCA shows only a very limited increase in *LWP* (Fig. 5f), HadGEM3-CLASSIC and CAM5-Oslo show a progressively more significant response whereas CAM5-NCAR shows a much larger response (Fig. 5h).

It is insightful to examine the influence of the eruption on precipitation in both observations and models using a similar analysis (Supplementary S10). We observe that there is little impact on precipitation indicating that the cloud system readjusts to a new equilibrium with little impact on either *LWP* or precipitation. The larger response in CAM5-NCAR ($\Delta LWP >$ 16 $g.m^{-2}$) is not supported by the MODIS observations where the 2002-2013 domain mean standard deviation in ΔLWP is ~4.5 $g.m^{-2}$. Thus, we are able to use the eruption to evaluate the models: HadGEM3 using UKCA and CAM5-Olso perform in a manner consistent with the MODIS observations while HadGEM3-CLASSIC and CAM5-NCAR do not. Moreover, the fact that changes in *LWP* are not detectable above natural variability suggests that aerosol-cloud interactions beyond the impact on r_{eff} are small (i.e. net second indirect effects are small).

The effective radiative forcing (ERF) from the event may be estimated from the difference between the top of atmosphere net irradiances from simulations including and excluding the volcanic emissions. The global ERF from HadGEM3 over the September-October 2014 period is estimated at -0.21 $W.m^{-2}$. Tests using an offline version of the radiation code reveal that the presence of overlying ice-cloud weakens the ERF by approximately 20% (Supplementary S11).

We also investigate whether a fissure eruption of this magnitude could have a more significant radiative impact if the timing/location of the eruptions were different (Supplementary S12). Our simulations suggest that for contrasting scenarios the global ERF would *i)* strengthen to -0.29 $W.m^{-2}$ (+40%) if the eruption commenced at the beginning of

June, *ii)* strengthen to -0.49 W.m^{-2} (+140%) if the fissure eruption had occurred in an area of South America where it could affect clouds in a stratocumulus-dominated regime, *iii)* strengthen to -0.32 W.m^{-2} (+55%) if the eruption had occurred in pre-industrial times when the background concentrations of aerosols was reduced[18] indicating that climatic impact of fissure eruptions such as Laki[41] in 1783-1784 would not have been as large if it had occurred in the present day.

Many studies[9,11,42,43] suggest that cloud adjustments may be dependent upon meteorological regime, so we ask whether the cloud *LWP* invariance observed near Holuhraun is simply a special case. We have reproduced the cloud regimes analysis derived from satellite measurements presented in a recent study[44]. We find that, when examining the 2014-15 eruption at Holuhraun, we are far from examining a meteorological 'special case', in fact rather the opposite (Supplementary S13); we are examining a region that contains the whole spectrum of liquid-dominated cloud regimes and deducing that, overall, the impact on *LWP* is minimal.

To further support our conclusion, we report results from a different event (Mount Kilauea, Hawaii, Supplementary S14), which degassing rate significantly increased during June-August 2008. The outflow of the plume affected the surrounding trade maritime cumuli[24,45,46], increasing the SW reflectance; the causal interpretations of this in the literature have varied[24,46]. affecting the surrounding trade maritime cumuli[24,45,46] and increased the SW reflectance in the outflow of the plume, although with different causal interpretations[24,46]. Again, *LWP* does not vary, either in the AMSR-E data[46] or in the MODIS monthly retrievals (Supplementary S14) which again suggests *LWP* insensitivity in the trade cumulus regime as well. Thus, for a very different meteorological environment dominated by very different cloud regimes, similar conclusions emerge.

4. Discussion and Conclusion (507 words of referenced text):

The 2014-15 eruption at Holuhraun presents a unique opportunity to investigate continental-scale aerosol-cloud climatic effects. Using synergistic observations and models driven by an empirical estimate of SO_2 emissions[33] we simulate spatial distributions of SO_2 that compare favourably with satellite observations. The HadGEM3 model is able to predict an impact from aerosol-cloud interactions of similar magnitude to the signal found in the MODIS data. Our analysis further highlights that cloud properties are largely unaffected by the eruption beyond the impact on r_{eff}.

We repeated the experiment with two additional GCMs and show that HadGEM3 using UKCA, CAM5-NCAR and CAM5-Oslo are able to capture the magnitude of the observed impacts on r_{eff} despite the lack of explicit representation of processes such as sub-cloud updraft velocities and entrainment, enhancing our confidence in GCMs' ability in predicting the aerosol first indirect effect. However, in line with recent work[16], modelled responses in the *LWP* differ significantly. The fact that cloud adjustments via *LWP* are not identified in the observations of the 2014-15 eruption at Holuhraun indicates that clouds are buffered against *LWP* changes[9-10,12], providing evidence that models with a low *LWP* response display a more convincing behaviour. These findings have wide scientific relevance in the field of climate modelling as, in terms of climate forcing, they suggest that aerosol second indirect effects appear small and climate models with a significant *LWP* feedback need reassessment[15-16,47].

Despite such massive emissions and large anomalies in r_{eff}, we estimate a moderate global-mean radiative forcing of -0.21 ± 0.08 $W.m^{-2}$ (1 standard deviation, Supplementary S15) for September-October which equates to a global annual mean effective radiative forcing of -0.035 ± 0.013 $W.m^{-2}$ (1 standard deviation) assuming that a forcing only occurs in September and October 2014. Global emissions of anthropogenic SO_2 currently total around 100 $TgSO_2$/year and the Intergovernmental Panel on Climate Change[17,47] suggests a best estimate for the aerosol forcing of -0.9 $W.m^{-2}$, yielding a forcing efficiency of -0.009 $W.m^{-2}/TgSO_2$. The emissions for September and October 2014 total approximately 4 $TgSO_2$, thus the global annual mean radiative forcing efficiency for the 2014-15 eruption at

Holuhraun yields a forcing efficiency of -0.0088 ± 0.0024 $W.m^{-2}/TgSO_2$ (1 standard deviation). The similarity is remarkable, but may be by chance given the modelled sensitivity to emission location and time (Supplementary S12).

Our study is not without caveats given that the observations themselves are uncertain owing to the limitations of satellite retrievals. The modelling is not completely constrained owing to the lack of detailed in-situ observations of e.g. the background aerosol concentrations and plume height. We cannot rule out that models showing small *LWP* sensitivity to aerosol emission behave as they do because they lack the resolution to represent fine-scale dynamical feedbacks[9,12]. Further high-resolution modelling of the 2014-15 Holuhraun eruption is necessary to evaluate more thoroughly how processes such as autoconversion or droplet evaporation plays a role in buffering the aerosol effect[9,12,48,49]. Bringing many of the different global models together and inter-comparing results of Holuhraun simulations is merited to provide a traceable route for reducing the uncertainty in future climate projections.

References:

[1]Twomey, S., The influence of pollution on the shortwave albedo of clouds. *J. Atmos. Sci.*, 34:1149–1152 (1977).

[2]Albrecht, B. A., Aerosols, cloud microphysics, and fractional cloudiness. *Science*, 245(4923):1227–1230 (1989).

[3]Haywood, J.M., and Boucher, O., Estimates of the direct and indirect radiative forcing due to tropospheric aerosols: a review. *Reviews of Geophysics*, 38, 513-543 (2000).

[4]Lohmann, U., Koren, I. and Kaufman, Y. J., Disentangling the role of microphysical and dynamical effects in determining cloud properties over the Atlantic. *Geophys. Res. Lett.*, 33, L09802, doi:10.1029/2005GL024625 (2006).

[5]Mauger, G. S., and J. R. Norris, Meteorological bias in satellite estimates of aerosol-cloud relationships. *Geophys. Res. Lett.*, 34, L16824, doi:10.1029/2007GL029952 (2007).

[6]Gryspeerdt, E., Quaas, J. and Bellouin, N., Constraining the aerosol influence on cloud fraction. *J. Geophys. Res. Atmos.*, 121, 3566–3583, doi:10.1002/2015JD023744 (2016).

[7]Ackerman, A. S. et al., The impact of humidity above stratiform clouds on indirect climate forcing. *Nature*, 432, 1014–1017 (2004).

[8]Sandu, I., J. L. Brenguier, O. Geoffroy, O. Thouron, and V. Masson, Aerosol impacts on the diurnal cycle of marine stratocumulus. *J. Atmos. Sci.*, 65, 2705–2718, doi:10.1175/2008JAS2451.1 (2008).

[9]Stevens, B. and Feingold, G., Untangling aerosol effects on clouds and precipitation in a buffered system. *Nature*, 461, 607–613 (2009).

[10]Seifert, A., Köhler, C., and Beheng, K. D., Aerosol-cloud-precipitation effects over Germany as simulated by a convective-scale numerical weather prediction model. *Atmos. Chem. Phys.*, 12, 709-725, doi:10.5194/acp-12-709-2012 (2012).

[11]Lebo, Z. J. and Feingold, G., On the relationship between responses in cloud water and precipitation to changes in aerosol. *Atmos. Chem. Phys.,* 14:11817–11831 (2014).

[12]Seifert, A., T. Heus, R. Pincus, and B. Stevens, Large-eddy simulation of the transient and near-equilibrium behaviour of precipitating shallow convection. *J. Adv. Model. Earth Syst.*, 7, 1918–1937, doi:10.1002/2015MS000489 (2015).

[13]Quaas, J. *et al.*, Aerosol indirect effects - general circulation model intercomparison and evaluation with satellite data. *Atmos. Chem. Phys.,* 9, 8697–8717, doi:10.5194/acp-9-8697-2009 (2009).

[14]Penner, J. E., Xu, L. & Wang, M. H., Satellite methods underestimate indirect climate forcing by aerosols. *Proc. Natl Acad. Sci.*, USA 108, 13404–13408, doi:10.1073/pnas.1018526108 (2011).

[15]Stevens, B., Rethinking the Lower Bound on Aerosol Radiative Forcing. *J. Clim.*, 28, 4794–4819, doi:10.1175/JCLI-D-14-00656.1 (2015).

[16]Ghan, S. *et al.*, Challenges in constraining anthropogenic aerosol effects on cloud radiative forcing using present-day spatiotemporal variability. *Proc. Natl. Acad. Sci. USA*, 113,5804–5811, doi:10.1073/pnas.1514036113 (2016).

[17]Boucher, O. *et al.*, Clouds and Aerosols. In: Climate Change 2013: The Physical Science Basis. Contribution of Working Group I to the Fifth Assessment Report of the Intergovernmental Panel on Climate Change [Stocker, T.F., D. Qin, G.-K. Plattner, M. Tignor, S.K. Allen, J. Boschung, A. Nauels, Y. Xia, V. Bex and P.M. Midgley (eds.)]. Cambridge University Press, Cambridge, United Kingdom and New York, NY, USA (2013).

[18]Carslaw, K. S. *et al.*, Large contribution of natural aerosols to uncertainty in indirect Forcing. *Nature*, 503(7474):67–71 (2013).

[19] Hamilton, D. S. *et al.*, Occurrence of pristine aerosol environments on a polluted planet. *Proceedings of the National Academy of Sciences of the United States of America*, doi:10.1073/pnas.1415440111 (2014).

[20] Lohmann, U. *et al.,* Total aerosol effect: radiative forcing or radiative flux perturbation?. *Atmos. Chem. Phys.,* 10, 3235-3246, doi:10.5194/acp-10-3235-2010 (2010).

[21] Gettelman, A., Putting the clouds back in aerosol-cloud interactions. *Atmos. Chem. Phys.,* 15:12397–12411, doi:10.5194/acp-15-12397-2015 (2015).

[22] McCormick, M.P., Thomason, L.W., and Trepte, C.R., Atmospheric effects of the Mt. Pinatubo eruption. *Nature*, v. 373, p. 399—404, doi:10.1038/373399a0 (1995).

[23] Gassó, S., Satellite observations of the impact of weak volcanic activity on marine clouds. *J. Geophys. Res.,* 113, D14S19, doi:10.1029/2007JD009106 (2008).

[24] Yuan, T., Remer, L. A., and Yu, H., Microphysical, macrophysical and radiative signatures of volcanic aerosols in trade wind cumulus observed by the A-Train. *Atmos. Chem. Phys.*, 11, 7119-7132, doi:10.5194/acp-11-7119-2011 (2011).

[25] Schmidt, A. *et al.*, Importance of tropospheric volcanic aerosol for indirect radiative forcing of climate. *Atmos. Chem. Phys.*, 12, 7321-7339, doi:10.5194/acp-12-7321-2012 (2012).

[26] Haywood, J. M., Jones, A. and Jones, G. S., The impact of volcanic eruptions in the period 2000–2013 on global mean temperature trends evaluated in the HadGEM2-ES climate model. *Atmos. Sci. Lett.*, 15: 92–96. doi:10.1002/asl2.471 (2014).

[27] Penner, J. E., C. Zhou, and L. Xu, Consistent estimates from satellites and models for the first aerosol indirect forcing. *Geophys. Res. Lett.*, 39, L13810, doi:10.1029/2012GL051870 (2012).

[28] Gettelman, A., A. Schmidt, and J.-E. Kristjánsson, Icelandic volcanic emissions and climate. *Nature Geoscience*, 8, 243, doi:10.1038/ngeo2376 (2015).

[29] McCoy, D. T., and D. L. Hartmann, Observations of a substantial cloud-aerosol indirect effect during the 2014–2015 Bárðarbunga-Veiðivötn fissure eruption in Iceland. *Geophys. Res. Lett.*, 42, 10,409–10,414, doi:10.1002/2015GL067070 (2015).

[30] Clarisse, L. *et al.*, Tracking and quantifying volcanic SO2 with IASI, the September 2007 eruption at Jebel at Tair. *Atmos. Chem. Phys.*, 8, 7723–7734, doi:10.5194/acp-8-7723-2008 (2008).

[31] Haywood, J.M. *et al.*, Observations of the eruption of the Sarychev volcano and simulations using the HadGEM2 climate model. *J. Geophys. Res.*, 115, D21212, doi:10.1029/2010JD014447 (2010).

[32]Schmidt, A. *et al.*, Satellite detection, long-range transport, and air quality impacts of volcanic sulfur dioxide from the 2014–2015 flood lava eruption at Bárðarbunga (Iceland). *J. Geophys. Res. Atmos.*, 120, doi:10.1002/2015JD023638 (2015).

[33]Thordarson, T., Self, S., Miller, D. J., Larsen, G., & Vilmundardóttir, E. G., Sulphur release from flood lava eruptions in the Veidivötn, Grímsvötn and Katla volcanic systems, Iceland. Geological Society, London, Special Publications, 213(1), 103-121 (2003).

[34]Polashenski, C. M. *et al.*, Neither dust nor black carbon causing apparent albedo decline in Greenland's dry snow zone: Implications for MODIS C5 surface reflectance. *Geophys. Res. Lett.*, 42, doi:10.1002/2015GL065912 (2015).

[35]Platnick, S. *et al.*, MODIS Atmosphere L2 Cloud Product (06_L2). NASA MODIS Adaptive Processing System, Goddard Space Flight Center, USA: http://dx.doi.org/10.5067/MODIS/MOD06_L2.006 (2015).

[36]Zhang, Z. and Platnick, S., An assessment of differences between cloud effective particle radius retrievals for marine water clouds from three MODIS spectral bands. *Journal of Geophysical Research: Atmospheres* (1984–2012), 116(D20) (2011).

[37]Stevens, B., and J-L Brenguier, Cloud Controlling Factors – Low Clouds, Heintzenberg, J., and R. J. Charlson, eds. Clouds in the Perturbed Climate System: Their Relationship to Energy Balance, Atmospheric Dynamics, and Precipitation. Strüngmann Forum Report, vol. 2. Cambridge, MA: MIT Press ISBN 978-0-262-01287-4 (2009).

[38]Bellouin, N. *et al.*, Aerosol forcing in the CMIP5 simulations by HadGEM2-ES and the role of ammonium nitrate. *J. Geophys. Res.*, doi:10.1029/2011JD016074 (2011).

[39]Dhomse, S. S. *et al.*, Aerosol microphysics simulations of the Mt. Pinatubo eruption with the UM-UKCA composition-climate model. *Atmos. Chem. Phys.*, 14, 11221-11246, doi: 10.5194/acp-14-11221-2014 (2014).

[40]Kirkevåg, A. et al., Aerosol-climate interactions in the Norwegian Earth System Model - NorESM1-M. *Geosci. Model Dev.*, 6, 207-244, doi:10.5194/gmd-6-207-2013 (2013).

[41]Schmidt, A. *et al.,* The impact of the 1783–1784 AD Laki eruption on global aerosol formation processes and cloud condensation nuclei. *Atmos. Chem. Phys.*, 10, 6025-6041, doi:10.5194/acp-10-6025-201 (2010).

[42]Zhang, S. *et al.*, On the characteristics of aerosol indirect effect based on dynamic regimes in global climate models. *Atmos. Chem. Phys.*, 16, 2765-2783, doi:10.5194/acp-16-2765-2016 (2016).

[43]Michibata, T., Suzuki, K., Sato, Y., and Takemura, T., The source of discrepancies in aerosol–cloud–precipitation interactions between GCM and A-Train retrievals. *Atmos. Chem. Phys.*, 16, 15413-15424, doi:10.5194/acp-16-15413-2016 (2016).

[44]Oreopoulos, L., N. Cho, D. Lee, and S. Kato, Radiative effects of global MODIS cloud regimes. *J. Geophys. Res. Atmos.*, 121, 2299–2317, doi:10.1002/ 2015JD024502 (2016).

[45]Eguchi, K. *et al.*, Modulation of cloud droplets and radiation over the North Pacific by Sulfate Aerosol Erupted from Mount Kilauea. *SOLA*, 7, 77–80, doi:10.2151/sola.2011-020 (2011).

[46]Mace, G. G., and A. C. Abernathy, Observational evidence for aerosol invigoration in shallow cumulus downstream of Mount Kilauea. *Geophys. Res. Lett.*, 43, 2981–2988, doi:10.1002/2016GL067830 (2016).

[47]Myhre, G. *et al.*, Anthropogenic and Natural Radiative Forcing. In: Climate Change 2013: The Physical Science Basis. Contribution of Working Group I to the Fifth Assessment Report of the Intergovernmental Panel on Climate Change [Stocker, T.F., D. Qin, G.-K. Plattner, M. Tignor, S.K. Allen, J. Boschung, A. Nauels, Y. Xia, V. Bex and P.M. Midgley (eds.)]. Cambridge University Press, Cambridge, United Kingdom and New York, NY, USA (2013).

[48]Golaz, J.-C., L. W. Horowitz, and H. Levy, Cloud tuning in a coupled climate model: impact on 20th century warming. *Geophys. Res. Lett.*, 40, 2246–2251, doi:10.1002/grl.50232 (2013).

[49]Zhou, C. and Penner, J. E.: Why do general circulation models overestimate the aerosol cloud lifetime effect? A case study comparing CAM5 and a CRM. *Atmos. Chem. Phys.*, 17, 21-29, doi:10.5194/acp-17-21-2017 (2017).

List of Supplementary Materials:

SUPPLEMENTARY_INFORMATION.docx

SI-Cloud-Animation.mp4

SI-SO2_animation.mp4

Acknowledgements: JMH, AJ, MD, BTJ, CEJ, JRK and FMOC were supported by the Joint UK BEIS/Defra Met Office Hadley Centre Climate Programme (GA01101). The National Center for Atmospheric Research is sponsored by the U.S. National Science Foundation. SB and LC are respectively Research Fellow and Research Associate funded by F.R.S.-FNRS. PS acknowledges support from the European Research Council (ERC) project ACCLAIM (Grant Agreement FP7-280025). JMH, FFM, DGP and PS were part funded by the UK Natural Environment Research Council project ACID-PRUF (NE/I020148/1). AS was funded by an Academic Research Fellowship from the University of Leeds and a NERC urgency grant NE/M021130/1 (The source and longevity of sulphur in an Icelandic flood basalt eruption plume). RA was supported by the NERC SMURPHS project NE/N006054/1. GWM was funded by the National Centre for Atmospheric Science, one of the UK Natural Environment Research Council's research centres. DPG is funded by the School of Earth and Environment at the University of Leeds. GWM and SD acknowledge additional EU funding from the ERC under the FP7 consortium project MACC-II (grant agreement 283576) and Horizon 2020 project MACC-III (grant agreement 633080). GWM, KSC and DG were also supported through the financial support via the Leeds-Met Office Academic Partnership (ASCI project). The work done with CAM5-Oslo is supported by the Research Council of Norway through the EVA project (grant 229771), NOTUR project nn2345k and NorStore project ns2345k. The following researchers have contributed substantially to the development version of CAM5-Oslo used in this study: Kari Alterskjær, Alf Grini, Matthias Hummel, Trond Iversen, Alf Kirkevåg, Dirk Olivié, Michael Schulz, Øyvind Seland. The AQUA/MODIS MYD08 L3 Global 1 Deg. dataset was acquired from the Level-1 and Atmosphere Archive & Distribution System (LAADS) Distributed Active Archive Center (DAAC), located in the Goddard Space Flight Center in Greenbelt, Maryland (https://ladsweb.nascom.nasa.gov/). This work is dedicated to the memory of Jón Egill Kristjánsson who died in a climbing accident in Norway. Jón Egill was a very active, talented and internationally respected researcher, and will be sadly missed.

Author contributions: FFM (Text, processing and analysis of the satellite data and the model results), JMH (Text, analysis of the satellite data and the model results, radiative transfer calculations), AJ, AG, IHHK and JEK (model runs), RA (processing of the CERES data and contribution to the text), LC and SB (processing of the IASI data and contribution to the text), LO, NC and DL (MODIS cloud regimes), DPG (estimate of CDNC from MODIS data), TT and MEH (provide emission estimates for the 2014-15 eruption at Holuhraun). AJ, NB, OB, KSC, SD, GWM, AS, HC, MD, AAH, BTJ, CEJ, FMOC, DGP, PS, (contribution to the development of UKCA), GM, SP, GLS, HT, JRK (discussion contributing to text and/or help with the MODIS data).

Author Information: The authors declare no competing financial interests. Correspondence and material requests should be addressed to Florent Malavelle (f.malavelle@exeter.ac.uk)

Figure legends:

Figure 1. The column loading of sulphur dioxide. *First column: processed data from HadGEM3 masked using positive detections of SO_2 from IASI and spatially and temporally coherent plume data from HadGEM3. Second column: processed data from IASI re-gridded onto the regular HadGEM3 grid. The column loading are expressed in Dobson Units (DU), with 1 DU equivalents to approximately 0.0285 $g[SO_2].m^{-2}$. In each case 'avg' represents the average concentration derived within the plume.*

Figure 2. Changes in cloud properties detected by MODIS AQUA for October 2014. *The mean changes in (a) cloud droplet effective radius (μm) and (c) liquid water path ($g.m^{-2}$) with corresponding zonal means. The probability distributions of absolute cloud droplet effective radius (b) and liquid water path (d) for the year 2014 (blue) and the 2002-2013 mean (green). Changes correspond to the deviation from the 2002-2013 mean. Stippling in a) and c) represent areas of 95% confidence level significant perturbation based on a two-tailed Student's t-test. Grey shading in the zonal means represent the standard deviation over 2002-2013.*

Figure 3. Changes in cloud properties modelled by HadGEM3 for October 2014. *The mean changes in (a) cloud droplet effective radius (μm) and (c) liquid water path ($g.m^{-2}$) with corresponding zonal means. The probability distributions of absolute cloud droplet effective radius (b) and liquid water path (d) for 2014 including (blue) or excluding (gold) the Holuhraun emissions, and the 2002-2013 mean (green). Changes correspond to the deviation from the 2002-2013 mean. Stippling in a) and c) represent areas of 95% confidence level significant perturbation based on a*

two-tailed Student's t-test. Grey shading in the zonal means represent the standard deviation over 2002-2013.

Figure 4. Modelled perturbations from HadGEM3 using UKCA during the Sept-Oct 2014 period. *Showing perturbations for a) AOD, b) N_d, c) r_{eff}, d) LWP, e) τ_{cloud}, and f) Top of Atmosphere (ToA) net SW radiation. Zonal means are shown for the 44°N-80°N, 60°W-30°E analysis region. The shaded regions represent the natural variability in the simulations from 2002-2013. Values outside of the light grey (respectively dark grey, bottom row) shaded regions represent significant perturbations at the 95% (respectively 67%) confidence level based on a two-tailed Student's t-test. Red lines represent HOL_{2014} minus NO_HOL_{2014} and blue lines represent HOL_{2014} minus $NO\_HOL_{2002\text{-}2013}$.*

Figure 5. Multi-model estimates of the changes in cloud properties for October 2014. *Left column shows Δr_{eff} (μm) and right column ΔLWP ($g.m^{-2}$) determined from HadGEM3 using the 2-moment UKCA/GLOMAP-mode aerosol scheme (first row), HadGEM3 using the single moment CLASSIC aerosol scheme (second row) CAM5-NCAR (third row), CAM5-Oslo (fourth row) and AQUA MODIS (last row). Note that MODIS anomalies show the aerosol impacts plus the meteorological variability while the model simulations show the impact of aerosols only (Supplementary S7).*

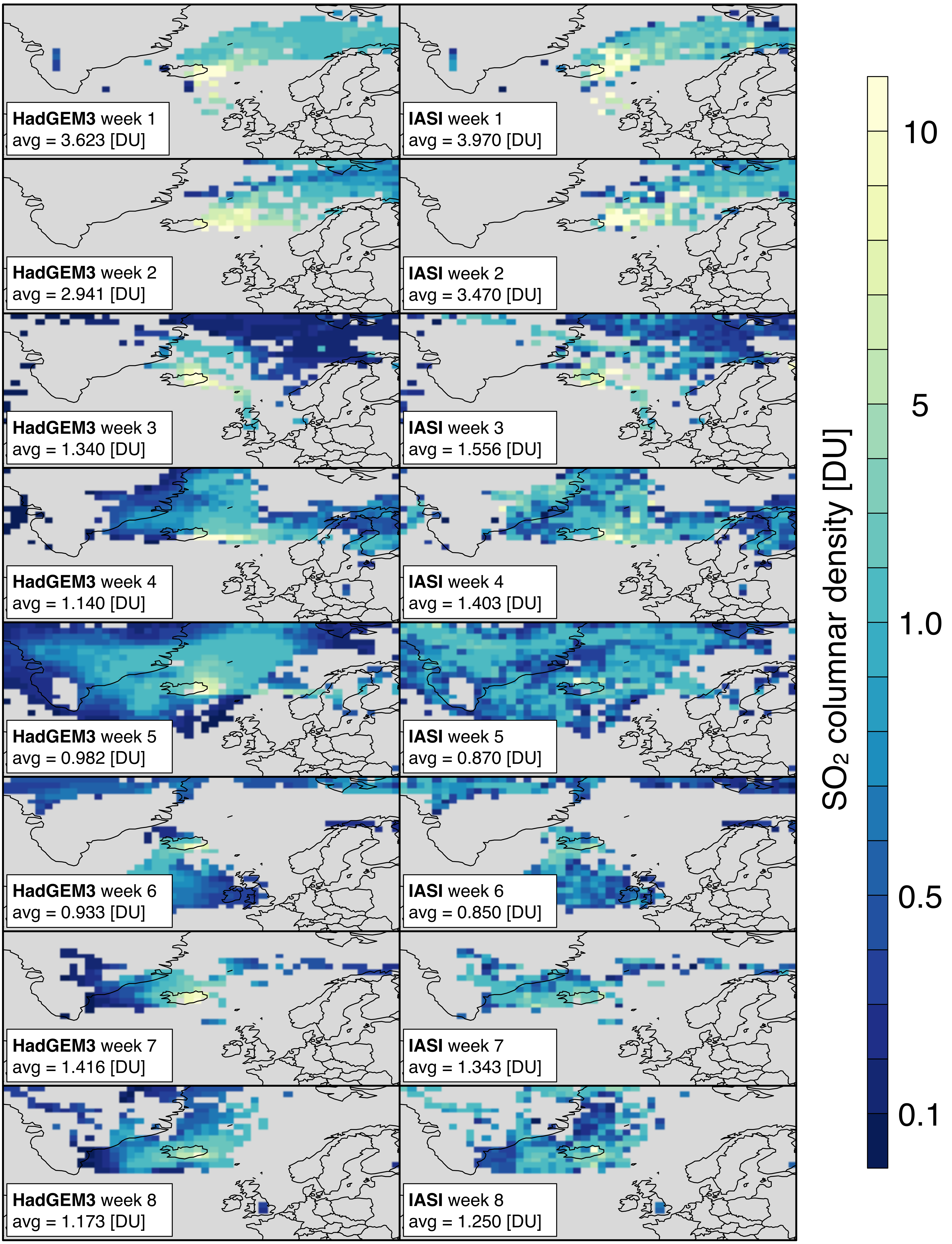
HadGEM3 week 1
avg = 3.623 [DU]
IASI week 1
avg = 3.970 [DU]
HadGEM3 week 2
avg = 2.941 [DU]
IASI week 2
avg = 3.470 [DU]
HadGEM3 week 3
avg = 1.340 [DU]
IASI week 3
avg = 1.556 [DU]
HadGEM3 week 4
avg = 1.140 [DU]
IASI week 4
avg = 1.403 [DU]
HadGEM3 week 5
avg = 0.982 [DU]
IASI week 5
avg = 0.870 [DU]
HadGEM3 week 6
avg = 0.933 [DU]
IASI week 6
avg = 0.850 [DU]
HadGEM3 week 7
avg = 1.416 [DU]
IASI week 7
avg = 1.343 [DU]
HadGEM3 week 8
avg = 1.173 [DU]
IASI week 8
avg = 1.250 [DU]
SO_2 columnar density [DU]
10
5
1.0
0.5
0.1

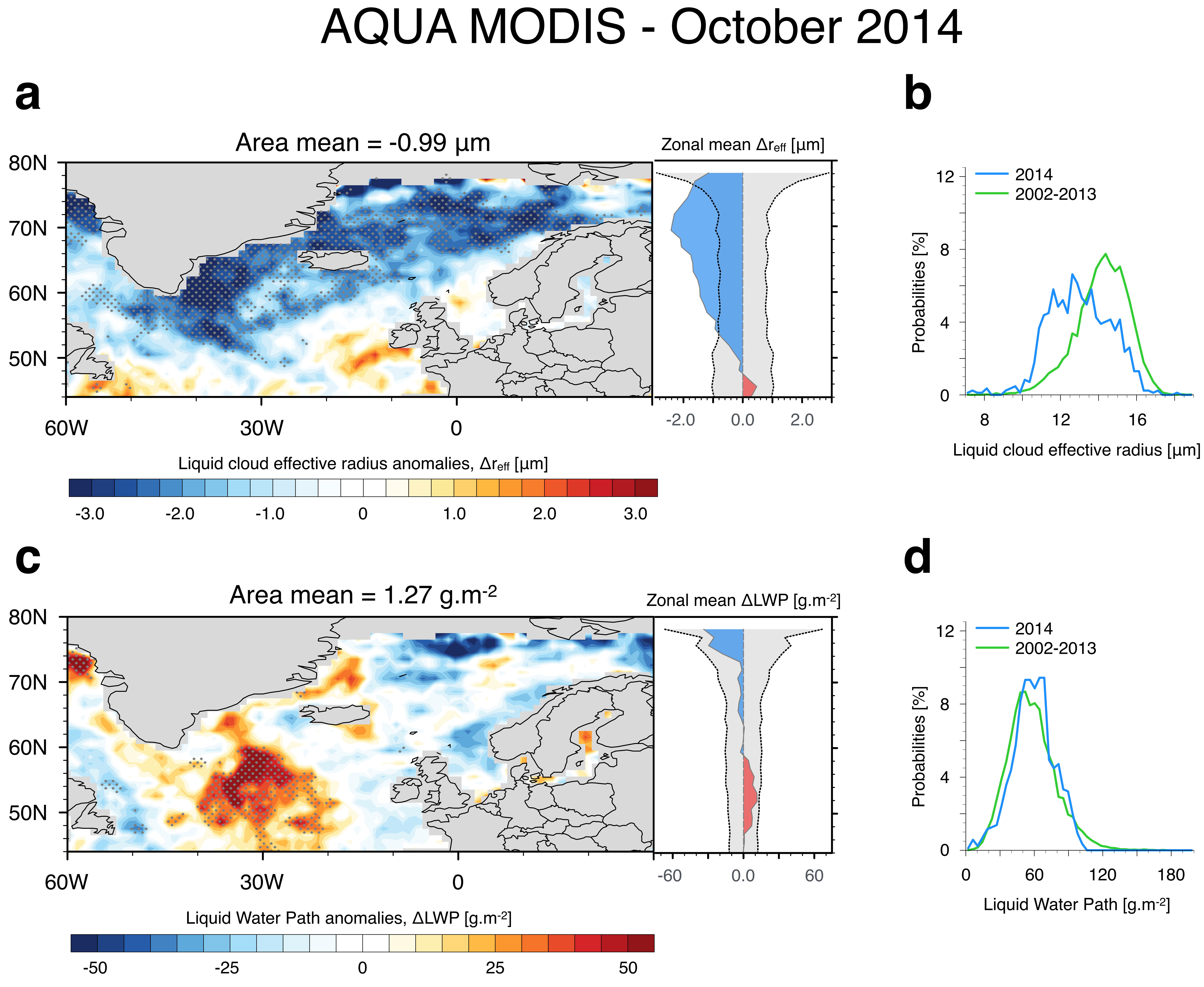
AQUA MODIS - October 2014
a
Area mean = -0.99 µm
Zonal mean Δreff [µm]
80N
70N
60N
50N
60W
30W
0
-2.0
0.0
2.0
Liquid cloud effective radius anomalies, Δreff [µm]
-3.0
-2.0
-1.0
0
1.0
2.0
3.0
b
2014
2002-2013
Probabilities [%]
12
8
4
0
8
12
16
Liquid cloud effective radius [µm]
c
Area mean = 1.27 g.m-2
Zonal mean ΔLWP [g.m-2]
80N
70N
60N
50N
60W
30W
0
-60
0.0
60
Liquid Water Path anomalies, ΔLWP [g.m-2]
-50
-25
0
25
50
d
2014
2002-2013
Probabilities [%]
12
8
4
0
0
60
120
180
Liquid Water Path [g.m-2]

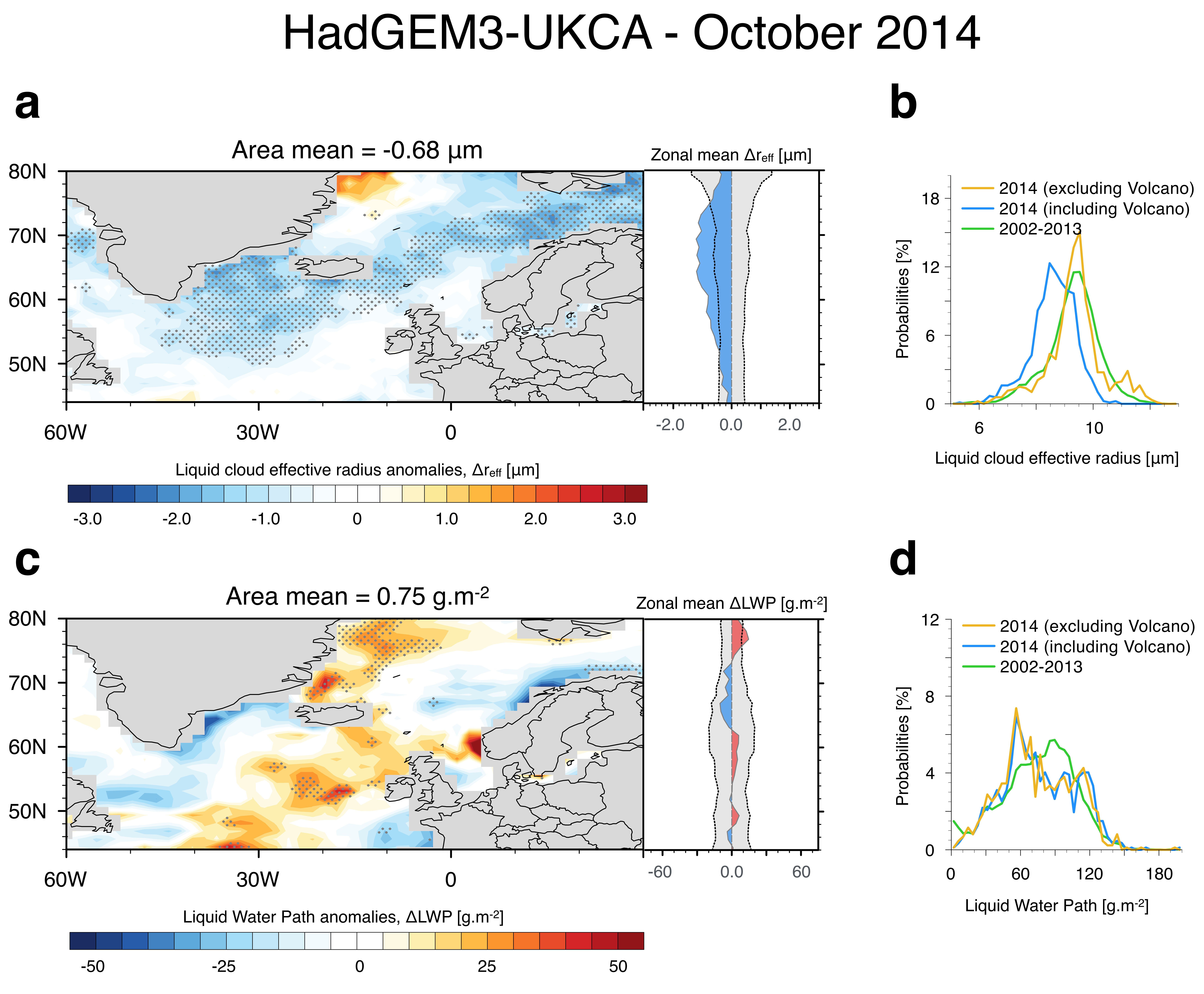

HadGEM3-UKCA - October 2014
a
Area mean = -0.68 µm
Zonal mean Δr_eff [µm]
80N
70N
60N
50N
60W
30W
0
-2.0
0.0
2.0
Liquid cloud effective radius anomalies, Δr_eff [µm]
-3.0
-2.0
-1.0
0
1.0
2.0
3.0
b
2014 (excluding Volcano)
2014 (including Volcano)
2002-2013
Probabilities [%]
18
12
6
0
6
10
Liquid cloud effective radius [µm]
c
Area mean = 0.75 g.m-2
Zonal mean ΔLWP [g.m-2]
80N
70N
60N
50N
60W
30W
0
-60
0.0
60
Liquid Water Path anomalies, ΔLWP [g.m-2]
-50
-25
0
25
50
d
2014 (excluding Volcano)
2014 (including Volcano)
2002-2013
Probabilities [%]
12
8
4
0
0
60
120
180
Liquid Water Path [g.m-2]

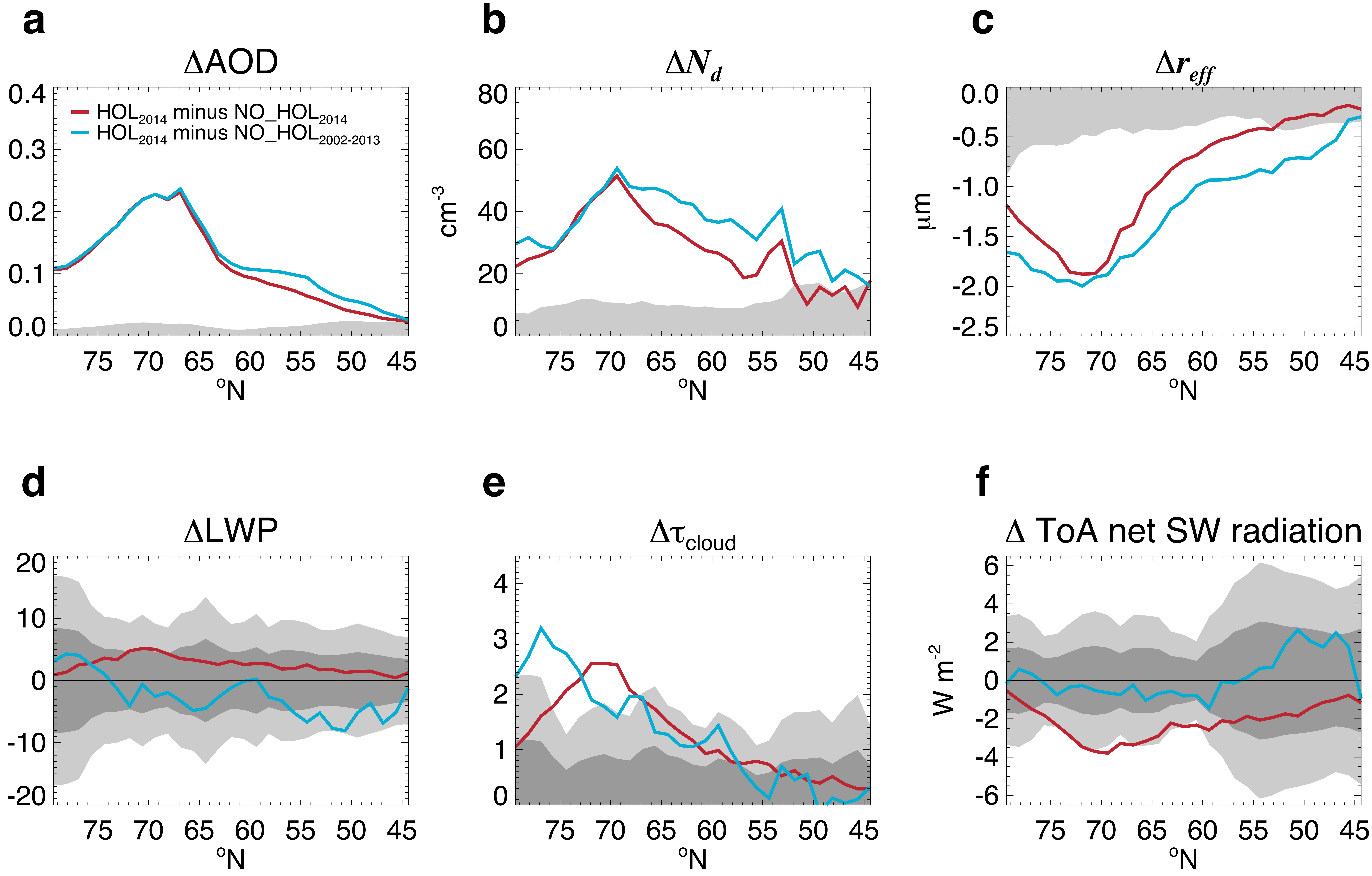
a
ΔAOD
HOL2014 minus NO_HOL2014
HOL2014 minus NO_HOL2002-2013
0.4
0.3
0.2
0.1
0.0
75 70 65 60 55 50 45
°N
b
ΔNd
cm-3
80
60
40
20
0
75 70 65 60 55 50 45
°N
c
Δreff
μm
0.0
-0.5
-1.0
-1.5
-2.0
-2.5
75 70 65 60 55 50 45
°N
d
ΔLWP
g m-2
20
10
0
-10
-20
75 70 65 60 55 50 45
°N
e
Δτcloud
4
3
2
1
0
75 70 65 60 55 50 45
°N
f
Δ ToA net SW radiation
W m-2
6
4
2
0
-2
-4
-6
75 70 65 60 55 50 45
°N

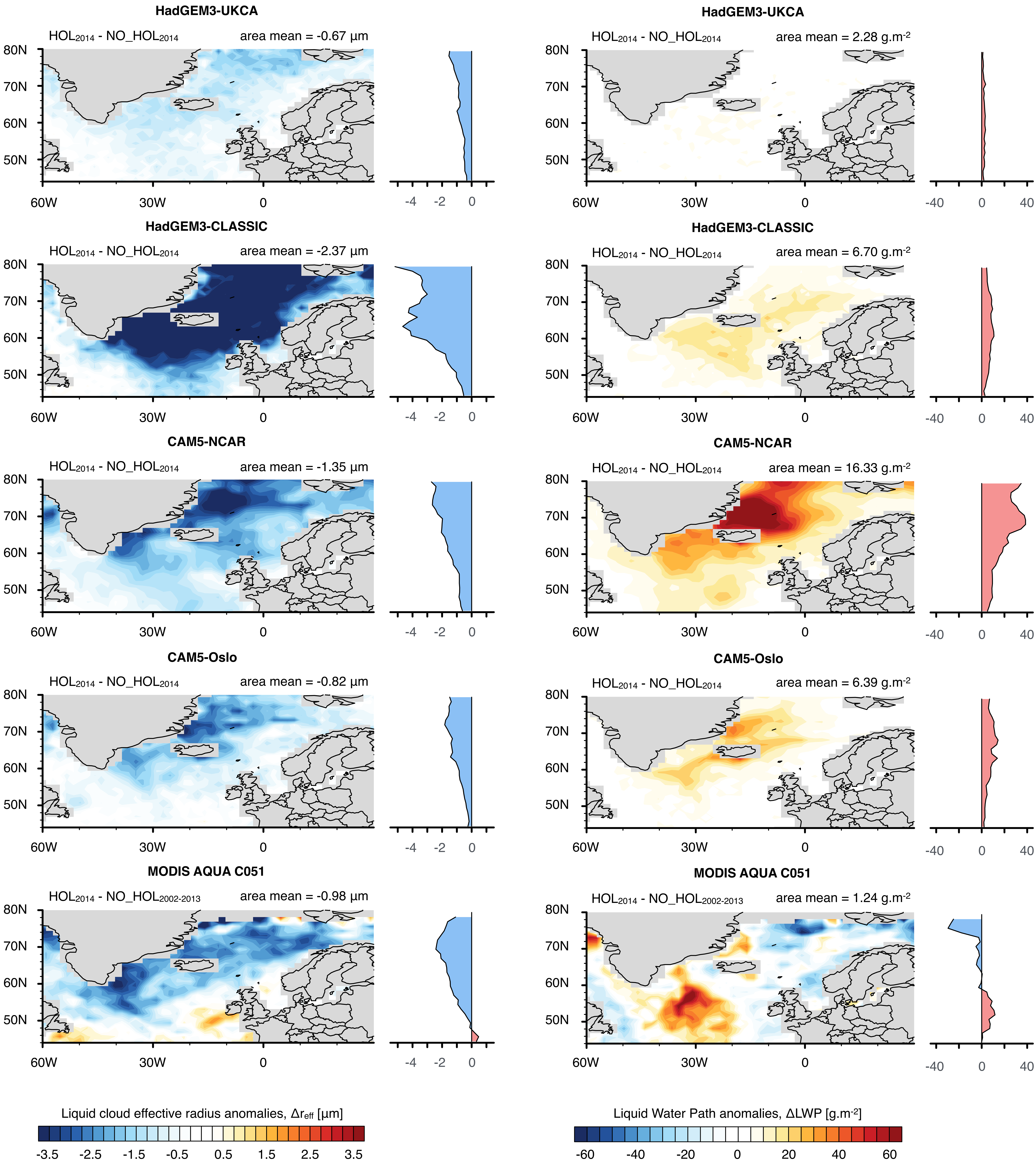
HadGEM3-UKCA
HOL2014 - NO_HOL2014
area mean = -0.67 µm
HadGEM3-UKCA
HOL2014 - NO_HOL2014
area mean = 2.28 g.m-2
HadGEM3-CLASSIC
HOL2014 - NO_HOL2014
area mean = -2.37 µm
HadGEM3-CLASSIC
HOL2014 - NO_HOL2014
area mean = 6.70 g.m-2
CAM5-NCAR
HOL2014 - NO_HOL2014
area mean = -1.35 µm
CAM5-NCAR
HOL2014 - NO_HOL2014
area mean = 16.33 g.m-2
CAM5-Oslo
HOL2014 - NO_HOL2014
area mean = -0.82 µm
CAM5-Oslo
HOL2014 - NO_HOL2014
area mean = 6.39 g.m-2
MODIS AQUA C051
HOL2014 - NO_HOL2002-2013
area mean = -0.98 µm
MODIS AQUA C051
HOL2014 - NO_HOL2002-2013
area mean = 1.24 g.m-2
80N
70N
60N
50N
60W
30W
0
-4
-2
0
-40
0
40
Liquid cloud effective radius anomalies, Δreff [µm]
-3.5
-2.5
-1.5
-0.5
0.5
1.5
2.5
3.5
Liquid Water Path anomalies, ΔLWP [g.m-2]
-60
-40
-20
0
20
40
60